Long-lasting restoration of memory function and hippocampal synaptic plasticity by focused ultrasound in Alzheimer's disease

Chanho Kong [a,1], Ji Woong Ahn [b,1], Sohyun Kim [b], Ji Young Park [a], Young Cheol Na [c], Jin Woo Chang [a], Seungsoo Chung [b,**], Won Seok Chang [a,*]

[a] Department of Neurosurgery, Yonsei University College of Medicine, Seoul, Republic of Korea
[b] Department of Physiology, Yonsei University College of Medicine, Seoul, Republic of Korea
[c] Department of Neurosurgery, Catholic Kwandong University College of Medicine, International St Mary's Hospital, Incheon, Republic of Korea

A R T I C L E   I N F O

A B S T R A C T

Background: Focused ultrasound (FUS) is a medical technology that non-invasively stimulates the brain and has been applied in thermal ablation, blood–brain barrier (BBB) opening, and neuromodulation. In recent years, numerous experiences and indications for the use of FUS in clinical and preclinical studies have rapidly expanded. Focused ultrasound-mediated BBB opening induces cognitive enhancement and neurogenesis; however, the underlying mechanisms have not been elucidated.

Methods: Here, we investigate the effects of FUS-mediated BBB opening on hippocampal long-term potentiation (LTP) and cognitive function in a 5xFAD mouse model of Alzheimer's disease (AD). We applied FUS with microbubble to the hippocampus and LTP was measured 6 weeks after BBB opening using FUS. Field recordings were made with a concentric bipolar electrode positioned in the CA1 region using an extracellular glass pipette filled with artificial cerebrospinal fluid. Morris water maze and Y-maze was performed to test cognitive function.

Results: Our results demonstrated that FUS-mediated BBB opening has a significant impact on increasing LTP at Schaffer collateral - CA1 synapses and rescues cognitive dysfunction and working memory. These effects persisted for up to 7 weeks post-treatment. Also, FUS-mediated BBB opening in the hippocampus increased PKA phosphorylation.

Conclusion: Therefore, it could be a promising treatment for neurodegenerative diseases as it remarkably increases LTP, thereby improving working memory.

1. Introduction

Focused ultrasound (FUS) (non-invasive brain stimulation method) is one of the most common multimodalities in the medical field. It can be easily inflected to control the function of the cortical areas without surgical intervention. In particular, low-intensity FUS with microbubbles (MB) can temporarily and reversibly open the blood–brain barrier (BBB), a specialized neurovascular structure that maintains homeostasis in the brain [1,2]. Since the BBB has selective ion permeability depending on their size or characteristics, the way we can deliver therapeutic agents into the brain is limited, but FUS with MB can open the BBB by increasing the delivery rate of drugs that cannot be delivered into the brain when treated alone. Many preclinical studies related to

this phenomenon have been conducted, and recently, many studies have been conducted on changes in inflammatory factors or neurotrophic factors through BBB opening many studies have been conducted on changes in inflammatory factors or neurotrophic factors through BBB opening [3–6]. In particular, FUS-mediated BBB opening (BBBO) has been reported to induce hippocampal neurogenesis, suggesting the possibility of treating diseases associated with cognitive decline, such as Alzheimer's disease (AD) [6–8]. Also, Recent research has shown that FUS reduces amyloid-β (Aβ) plaques [9–11], and the safety of BBBO in patients with Alzheimer's disease has been verified [12–14].

AD is a multifactorial neurodegenerative disorder characterized by abnormal thinking and behavioral disorders due to progressive cognitive decline, memory loss, and synaptic dysfunction. Typical

pathological characteristics of AD include Aβ plaques and neurofibrillary tangles of tau protein [15–17]. In a preclinical study on FUS for AD, anti-Aβ antibodies were delivered to the brain by increasing the permeability of the BBB. It resulted in increases of binding efficacy to Ab plaques, rapidly reducing plaque pathology [18]. Since then, research on using FUS-mediated BBBO to facilitate the delivery of therapeutic agents in AD patients has gained attention [19–22]. Notably, studies have reported that amyloid pathology and phosphorylated tau can be reduced solely by FUS-induced BBB opening without specific drug delivery [23,24]. In animal models of AD, FUS-mediated BBBO has also been shown to affect memory recovery [10,25–27]. Ongoing research is investigating various biological changes induced by FUS-mediated BBBO. However, in order to be a promising non-pharmacological treatment method for AD, further research is necessary to understand why amyloid is reduced and cognitive function is restored.

Severe impairment in the induction of synaptic plasticity, including gradual inhibition of long-term potentiation (LTP), a decrease in spontaneous firing rate, and excitatory postsynaptic potential (EPSP) of hippocampal neurons, are important mechanisms closely involved in learning and memory [28,29]. Therefore, preventing synaptic loss and preserving, improving, or restoring synaptic function in neurons is a promising therapeutic approach for controlling or alleviating cognitive impairment in patients with Alzheimer's disease. In our study, we confirmed changes in LTP by FUS-mediated BBBO. The improvement in cognitive function caused by FUS-mediated BBBO is already known, but the underlying mechanism has not been revealed. Therefore, we investigated whether the long-term strengthening effect of synapses actually occurs by examining alterations in hippocampal LTP after FUS-mediated BBBO. This study suggests that FUS can open the BBB of the rodent hippocampus, resulting in the restoration of cognitive deficits caused by Alzheimer's disease in rodent models. The underlying synaptic mechanisms were investigated, which led to the potential application of therapeutic focused ultrasound in the brain, with emphases on its current emerging clinical implications.

2. Materials and methods

2.1. Animals

We obtained transgenic mice with 5XFAD from the Jackson Laboratories. The mice overexpressed mutant human amyloid beta (A4) precursor protein 695 (APP) with Swedish (K670 N, M671L), Florida (I716V), and London (V717I) familial Alzheimer's disease (FAD) mutations combined with human presenilin1 (PS1) harboring two FAD mutations, M146L and L286V. We verified constructed transgenic mice using PCR and used non-transgenic littermates (LM) as the control group. The 5xFAD mice exhibit extracellular amyloid deposition beginning at approximately 2 months, first in the subiculum and then in the internal pyramidal layer of the cortex. The Aβ42 also accumulated intraneuronally in an aggregated form within the soma and neuritis starting at 1.5 months. In addition, basal synaptic transmission and LTP in the hippocampal CA1 region began to deteriorate between 4 and 6 months. In general, we detected memory impairment from 4 to 6 months of age. We conducted all animal experimental procedures in compliance with the Guide for Care and Use of Laboratory Animals of the National Institution of Health. The study design was approved by the Institutional Animal Care and Use Committee (IACUC; 2020–0251) of Yonsei University. The mice were housed one per cage and maintained with food and water available ad libitum on a 12-h light/dark cycle (lights on at 8 a.m. and off at 8 p.m.) in a temperature-controlled environment (23 ± 2 °C).

2.2. Focused ultrasound equipment

We used a 0.5 MHz single element focused transducer (H-107MR; SonicConcepts, Bothell, WA, USA) with a diameter of 51.7 mm and

radius of curvature of 63.2 mm. The transducer was assembled with a polycarbonate coupling cone, and the cone was filled with degassed water for acoustic energy efficiency. We connected a waveform generator (33220A, Agilent, Palo Alto, CA, USA) to a 50 dB Radio Frequency power amplifier (240 L, ENI Inc., Rochester, NY, USA) to drive the FUS transducer, and used a power meter (E4419B, Agilent) to measure the input electrical power. We matched the electrical impedance of the transducer to the output impedance (50 Ω) of the amplifier using an external matching network (Sonic Concept Inc., Bothell, WA, USA).

2.3. Stereotaxic surgery

We randomly weighed and housed male 5xFAD (6–7 months old, 20–30 g) in cages. The animals were divided into five groups: Sham, Sham + FUS, transgenic (TG), TG + FUS, and Naïve groups. All mice were anesthetized with isoflurane (2.5% for induction, 1–1.5% for maintenance in 70% nitrous oxide and 30% oxygen), and the animals' heads were fixed on a stereotaxic frame (Narishige, Tokyo, Japan). We used a medical sterile ultrasound gel (ProGel-Dayo Medical Co, Seoul, South Korea) to fill the space between the coupling cone filled with degassed water and the skull for energy transfer efficiency. DEFINITY microbubbles (0.04 ml/kg; Lantheus Medical Imaging, North Billerica, MA, USA) were injected intravenously after confirming the coordinates of the target point on the skull, and sonication (1-Hz burst repetition frequency, 10-ms bursts, 120 s in total, average peak pressure 0.25 MPa) was initiated at the same time. We applied FUS sonication to the bilateral hippocampus (anteroposterior [AP] = −1.4 mm from bregma; mediolateral [ML] = ± 1.2 mm; AP = −2.4 mm from bregma, ML = ± 2.2 mm). All groups underwent the following procedure: anesthesia with isoflurane, fixing the head with a stereotactic frame, skin incision, locating the transducer right on the skull, and intravenously injecting microbubbles.

2.4. Magnetic resonance imaging

We performed magnetic resonance imaging (MRI) immediately after sonication with a Bruker 9.4 T 20 cm bore MRI system (Biospec 94/20 USR; Bruker, Ettlingen, Germany) and a mouse head coil. A gadolinium-based MRI contrast agent, Gadobutrol (Gd; Gadovist; 0.2 ml/kg), was injected intravenously. To confirm the permeability of the BBB, we compared post-T1 weighted images with gadolinium to pre-T1 weighted images without gadolinium (Fig. 1B).

2.5. Hippocampal slice preparation

To perform field recordings, mice were sacrificed after 6 weeks of FUS treatment (Fig. 1A). Hippocampal slices (400 μm thick) were prepared from TG mice with or without FUS treatment. The mice were anesthetized with isoflurane (5% isoflurane, 95% O_2) and perfused with ice-cold sucrose artificial cerebrospinal fluid (aCSF) at the following concentrations in mM: 195.5 sucrose, 2.5 KCl, 1 NaH_2PO_4, 32.5 $NaHCO_3$, 11 glucose, 2 Na pyruvate, and 1 Na ascorbate (all chemicals from Sigma-Aldrich, St. Louis, MO, USA) bubbled with 95% O_2/5% CO_2 at a pH of 7.4. After perfusion, the brains were quickly removed from the skull and the slices cut on a vibratome (Leica Biosystems, Wetzlar, Germany) and transferred to an incubation chamber containing incubation solution with the following concentrations in mM: 119 NaCl, 2.5 KCl, 1 NaH_2PO_4, 26.2 $NaHCO_3$, 11 glucose, 2 Na pyruvate, 1 Na ascorbate, 3 $MgSO_4$, and 1.5 $CaCl_2$ at 35 °C for 15 min. After incubation, we transferred the slices to a container filled with a CSF solution at 23–24 °C for 1 h.

2.6. Electrophysiology

Field recordings were performed with a concentric bipolar electrode positioned in the stratum radiatum of the CA1 region using an
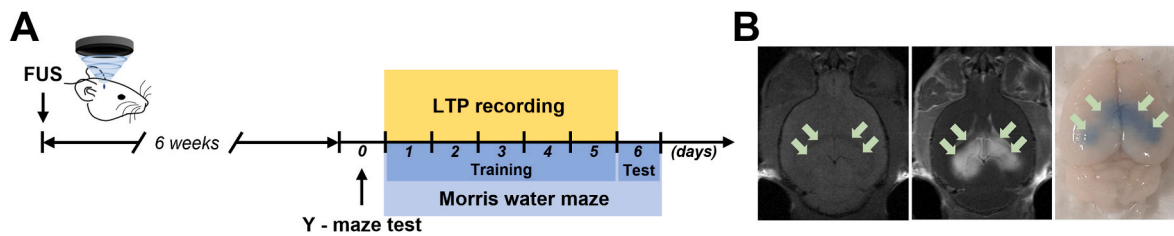
Fig. 1. Schematic of experimental design. A, Experimental timeline: After 6 weeks of FUS treatment, LTP measurement and behavioral experiments were performed. **B,** T1-weighted pre-/post-contrast MR images were taken to confirm the increase in BBB permeability. 4 target regions (arrow) of the hippocampus were sonicated.

extracellular glass pipette (3–5 MΩ) filled with aCSF. Stimulation was delivered through a bipolar electrode (FHC; Bowdoin, ME, USA) placed in the Schaffer collateral-CA1 (SC). The SC circuit was visualized using differential interference contrast (DIC) microscopy at $4 \times$ magnification and identified by the ability to evoke short and constant latency field excitatory postsynaptic potentials (fEPSPs) at CA1 synapses by SC input stimulation. We measured the test stimulation in all fEPSP experiments prior to the beginning of all experiments (30–300 μA) and used a test pulse stimulation strength that evoked 50% of the maximum fEPSP. We recorded baseline synaptic responses for 30 min, and induced LTP by high-frequency stimulation (HFS; 100 Hz, 4 trains, 1 s duration, 20 s inter-train interval). Recordings were made every 10 s for 1 h using the Axopatch 1D amplifier (Molecular Devices, Sunnyvale, CA, USA) that was digitized at 10 KHz and filtered at 2 KHz with Digidata 1322A and pClamp 10.0 software (Molecular devise, Sunnyvale, CA, USA). The electrode was filled with an internal solution (concentration in mM: 135 Cs methanesulfonate, 8 NaCl, 10 HEPES, 0.5 EGTA, 4 Mg-ATP, 0.3 Na-GTP, and 5 QX-315 Cl; pH 7.25 with CsOH, 285 mOsm) to measure excitatory postsynaptic currents (EPSCs). The currents were recorded in the presence of tetrodotoxin (1 μM TTX, Tocris, Bristol, England) to block sodium currents and propagate action potentials. We recorded spontaneous firing in cell-attached mode from the CA3 principal cells and stratum radiatum interneurons.

2.7. Morris water maze test

We performed a water maze test 6 weeks after FUS treatment to verify the improvement in cognitive function by FUS. A circular water pool (12 cm in diameter) was filled with water (23 ± 2 °C temperature), and the water was mixed with edible dye (Bright White Liqua-Gel; Chefmaster, CA, USA) to make it opaque so that the platform (10 cm in diameter) was not visible. Visual cues of different shapes were marked on the walls of the four quadrants, North (N), West (W), South (S), and East (E), of the pool. Water was filled up to 1 cm above the platform, placed at the center of one (SW) of the four quadrants. Learning training to remember the platform was performed for 5 consecutive days, and probe tests were performed on the 6th day. All mice were trained to remember the platform for 5 days, four times a day, and the probe test was performed on the 6th day. The subjects were placed into four quadrants facing the wall and allowed 1 min to reach the platform. Mice that found the platform within 1 min were left on the platform for 10 s for learning, and those that did not be find it were placed on the platform for 10 s. The probe test was performed after removing the platform. The mice started on the wall of the quadrant zone opposite to the platform, and their movements for 1 min were recorded using a tracking system (Harvard Apparatus, Holliston, MA, USA).

2.8. Spontaneous alteration Y-maze test

To investigate cognition and spatial memory, spontaneous alternation test in the Y-maze was investigated in the mice. We performed the Y-maze test 6 weeks after FUS treatment (Fig. 1A). The alternation performance was performed using an asymmetric Y-maze, consisting of three identical arms (15 cm high × 9 wide cm × 40 cm long), and

constructed using black acrylic material. All animals were placed in the center of the Y-maze and allowed to explore freely for 8 min. All the routes of movement were recorded and calculated using a video camera and analyzed to determine the percentage of alternation by manually evaluating the number of triads containing entries into all three arms.

2.9. Immunohistochemistry

All animals that underwent the behavioral experiment were sacrificed for brain tissue collection after the behavioral test. Animals were anesthetized using an intraperitoneal injection of ketamine and xylazine, followed by perfusion with 0.9% saline and 4% paraformaldehyde (PFA). The extracted brains were fixed in 4% PFA for 24 h and kept in a 30% sucrose solution for approximately 3 days. Brains were cut into 30 μm coronal sections. Free-floating sections were washed in PBS and incubated in blocking solution (PBS, 5% normal goat serum, 0.2% Triton X100) for 1 h at room temperature. The sections were incubated with primary antibodies in blocking solution overnight at 4 °C. The following primary antibodies were used for immunohistochemistry: 6E10 (anti-human Aβ monoclonal antibody, BioLegend, SIG39320, mouse, 1:500). After the primary immunoreaction, the sections were incubated with secondary antibodies conjugated with Alexa 594 (Abcam, A150156, 1:250). Immunostaining of the sections was visualized using an Axio Imager M2 light microscope (Carl Zeiss). The plaque area detected by 6E10 was quantified using the ImageJ software (version 1.52a, Wayne Rasband, NIH, MD, USA).

2.10. Western blot analysis

Tissue samples from the hippocampus were homogenized in lysis buffer (PRO-PREP; iNtRON Biotechnology, South Korea) with a protease and phosphatase inhibitor cocktail mix (Protease/Phosphatase inhibitor cocktail, 5872, Cell Signaling, London, UK). The protein concentration was measured using a Pierce BCA Protein Assay Kit (Thermo Fisher, USA). Twenty micrograms of each protein were separated on a 12% SDS–PAGE gel and subsequently transferred to an Immun-Blot PVDF membrane (Bio-Rad, USA). Membranes were placed in blocking buffer (5% bovine serum albumin or 5% powdered skim milk in TBST) for 1 h at room temperature and then incubated with primary antibody at 4 °C overnight. The primary antibodies used were as follows: GAPDH (Cell Signaling, Denver, MA, USA, #2118, 1:2000), PKA (Cell Signaling, Denver, MA, USA, #4782, 1:1000) and Phospho-PKA (Thr197) (Cell Signaling, Denver, MA, USA, #4781, 1:1000). Following three times 5-min washing with TBST, the membranes were incubated with the corresponding secondary antibodies for 90 min at room temperature with goat anti-rabbit IgG(H + L)-HRP (GenDEPOT, Katy, TX, USA). The proteins were visualized using an enhanced chemiluminescence solution (West Save Gold, AbFrontier Inc., Korea), and the blots were analyzed using an Amersham ImageQuant 800 Western blot imaging station (Cytiva; USA). Band intensities were quantified using an analysis system (Multi Gauge version 3.0, Fujifilm, Tokyo, Japan).

2.11. Statistical analysis

All data were expressed as mean ± standard error of the mean (SEM). All statistical analyses were performed using the statistical package fir the social sciences (SPSS) version 20 (SPSS Inc., Chicago, IL, USA) and GraphPad Prism 8 software (GraphPad Software Inc., San Diego, CA, USA). Comparisons between two groups were performed using the Student's t-test. Most results were statistically analyzed using one-way analysis of variance (ANOVA) followed by Tukey's post-hoc test. As an exception, comparisons between groups over days in the MWM training were analyzed by two-way ANOVA with Fisher's least significant difference post-hoc test for preplanned multiple comparisons when appropriate. Data for Aβ quantification were analyzed using unpaired *t*-test (two-tailed). For all analyses, statistical significance was set at $p < 0.05$.

3. Results

3.1. Restoration of memory impairment by FUS

The Morris water maze test was performed to investigate changes in cognitive function and memory following FUS-mediated BBB opening in the four groups: Sham (n = 11), Sham + FUS (n = 11), TG (n = 6) and TG + FUS (n = 6). Throughout the five days of training, the time to find the platform gradually decreased, except in the TG group (Fig. 2A). In contrast, the TG group spent more time searching for and reaching the platform, indicating that they had difficulties with learning and memory. Sham (31.37 ± 4.89 s, $p < 0.05$) and Sham + FUS (30.37 ± 4.89 s, $p < 0.05$) groups showed significantly better memory and learning abilities than the TG group on the second day of training (Fig. 2A). During the training until the 5th day, the latency to platform gradually decreased in the Sham (Day 3, 28.5 ± 5.0 s, $p < 0.05$; Day 4, 20.9 ± 4.2 s, $p < 0.01$; Day 5, 22.90 ± 4.0 s, $p < 0.01$) and Sham + FUS (Day 3, 25.6 ± 5.2 s, $p < 0.05$; Day 4, 22.2 ± 5.6 s, $p < 0.05$; Day 5, 22.7 ± 4.5 s, $p < 0.01$) groups compared to the TG group (Fig. 2A). The TG + FUS group (Day 1, 49.6 ± 3.3 s; Day 2, 45.5 ± 5.36 s; Day 3, 33.6 ± 5.8 s, Day 4, 30.1 ± 8.9 s; Day 5, 26.4 ± 6.3 s, $p < 0.01$) gradually learned about memory, and there was a significant difference compared with the TG group (Day 1, 47.6 ± 4.3 s; Day 2, 47.3 ± 6.3 s; Day 3, 45.4 ± 6.8 s; Day 4, 42.3 ± 7.25 s; Day 5, 46.8 ± 5.3 s) on the 5th day of training (Fig. 2A). On day 6, the platform in the pool was removed and a probe test was performed (Fig. 2B–F). The TG group had significantly fewer number of crossings (0.3 ± 0.2, $p < 0.05$) and time spent in the target quadrant zone (5.8 ± 1.6 s, $p < 0.01$) than the sham group (crossings, 3.2 ± 0.7; quadrant zone, 17.0 ± 1.7 s) (Fig. 2C–D). In contrast, the number of crossings across the platform zone (3.5 ± 0.9, $p < 0.05$), time spent in the target quadrant zone (23.2 ± 3.7 s, $p < 0.05$), and time spent in the platform zone (1.2 ± 0.2 s, $p < 0.05$) were significantly higher in the TG + FUS group than in the TG group (crossings, 0.3 ± 0.2; quadrant zone, 5.8 ± 1.6 s; platform zone, 0.05 ± 0.04 s) (Fig. 2D–E). In terms of movement, the movement speed of the TG group was slower than that of the Sham and Sham + FUS group (Sham, 20.5 ± 1.17 cm/s, $p < 0.05$; Sham + FUS, 19.2 ± 0.78 cm/s, $p < 0.05$; TG, 12.9 ± 2.8 cm/s; TG + FUS, 19.9 ± 2.2 cm/s) (Fig. 2F).

To investigate the effect of FUS on cognitive impairment in 5xFAD mice, we assessed spatial memory among the four groups using the Y-maze test as follows: Sham (n = 14), Sham + FUS (n = 13), TG (n = 9) and TG + FUS (n = 10) (Fig. 2G). The Sham (65.5 ± 3.4%, $p < 0.01$) and Sham + FUS (64.3 ± 3.4%, $p < 0.01$) groups showed the expected alternation rate and avoiding the formerly entered arms, whereas the TG group (43.8 ± 5.4%) showed altered chance by visiting formerly entered arms. However, the TG + FUS group (61.4 ± 2.4%, $p < 0.05$) showed improved alternation compared to the TG group (Fig. 2H). The total number of arm entries used to evaluate locomotion and activity is shown in Fig. 2I. The results showed that FUS-mediated BBB opening significantly increased spontaneous alternation in the Y-maze test.

3.2. Changes the synaptic strength and LTP

The changes in functional outcome after FUS treatment were assessed by electrophysiological experiments to measure synaptic strength and LTP. LTP measurements were performed by dividing the groups into Naive (10 slices/5 mice), Sham (slices/5 mice), Sham + FUS (11 slices/5 mice), TG (12 slices/5 mice) and TG + FUS (9 slices/4 mice). Bilateral hippocampal tissues were obtained from one subject. The effect of FUS on hippocampal synaptic plasticity in APP-TG mice was investigated. The synaptic strengths of individual mice were recorded as fEPSPs in the SC-CA1 circuits in acute hippocampal brain slices (Fig. 3N). Synaptic strength was profoundly reduced in APP TG mice compared to naïve or littermates (LM) of the same age. However, synaptic strength was remarkably recovered in APP TG mice after FUS treatment (Fig. 3A–E). We compared the synaptic strengths in each group by measuring the slopes of the Input and Output (I/O) relationships (I/O slopes) obtained in Fig. 3F–G. The slope of the I/O relationship was analyzed by plotting the initial slope of the evoked AMPAR fEPSPs versus the fiber volley amplitude (an indicator of afferent fiber recruitment) over a range of stimulus intensities. The effects of FUS on LTP induction were also investigated. According to the *ex vivo* results obtained from the acute hippocampal slices of APP TG mice fed FUS, the depressed LTP was significantly improved in APP TG mice to the level of naïve and LM of the same age (Fig. 3H–M). Thus, our results confirmed that FUS improved cognitive impairments by restoring long-term synaptic strength almost fully in APP TG mice by modulating hippocampal plasticity with improved LTP induction.
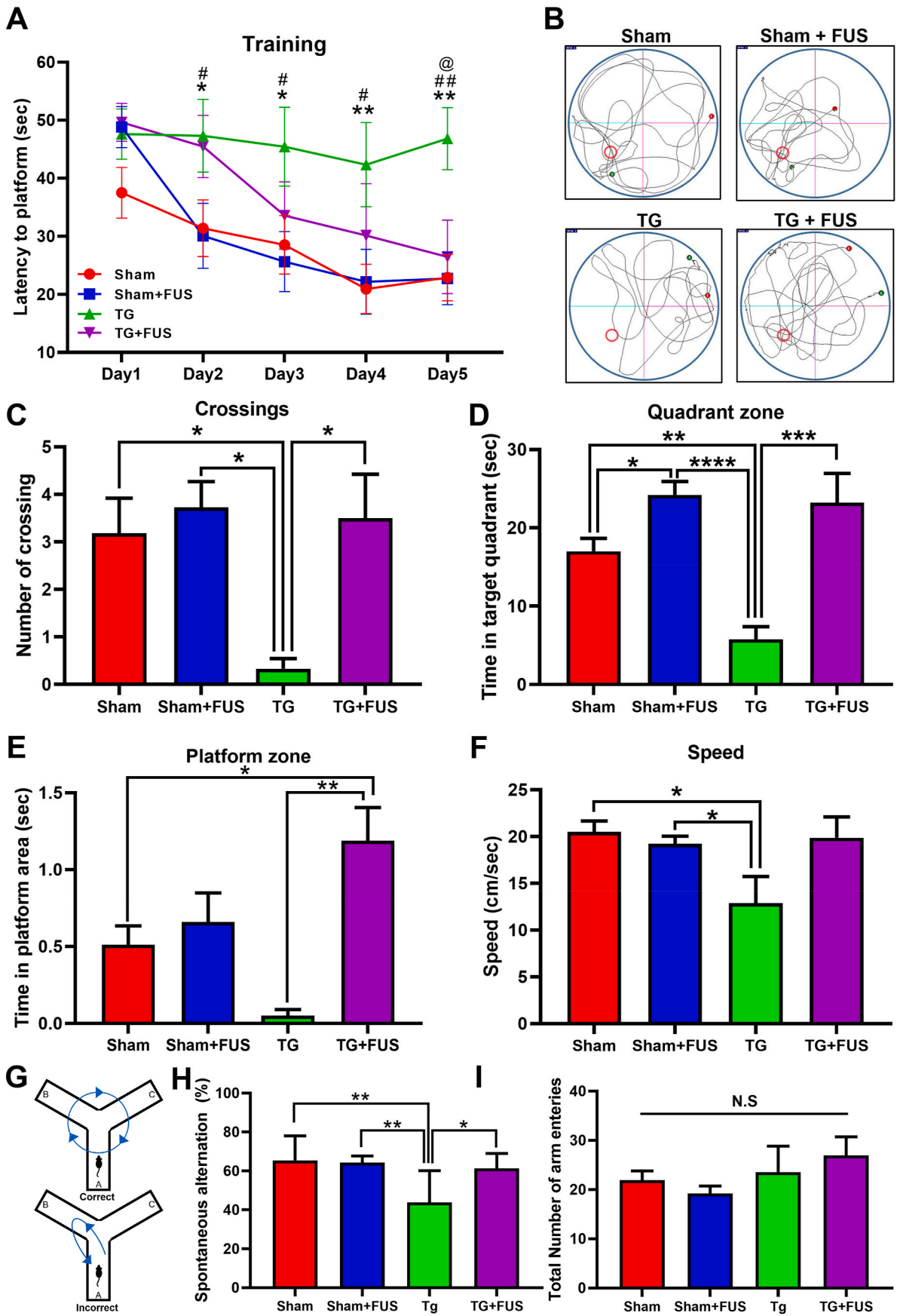
3.3. Changes of Aβ in the hippocampus

To confirm whether the Aβ reduction effect of FUS lasted up to 7 weeks, the Aβ marker 6E10 was stained (Fig. 4A). Amyloid-β was quantified in the dentate gyrus (DG) of the hippocampus, targeting FUS energy. As a result, no significant differences were found in the total area of the Aβ plaques in the DG of the hippocampus in the TG + FUS group (10,018.6 ± 918.4 μm^2, n = 5) compared to the TG group (8601.4 ± 1838.5 μm^2, n = 4) (Fig. 4B).

3.4. Changes of the PKA expression

We assessed whether the phosphorylation of PKA protein levels was altered in the hippocampus of the TG mice relative to those in the control hippocampus. We divided the rats into Sham (n = 8), Sham + FUS (n = 9), TG (n = 9), and TG + FUS (n = 9) groups and performed western blotting. Western blot analysis showed marked increase in p-PKA/PKA levels in the TG + FUS group (0.85 ± 0.03) relative to those in the TG group (0.66 ± 0.04). The TG group exhibited a significantly reduced expression level of PKA in the hippocampus compared to the Sham (0.89 ± 0.06) and Sham + FUS (0.96 ± 0.06) groups (Fig. 5A–B). These findings indicate that FUS-mediated BBB opening in the hippocampus increased PKA phosphorylation.

4. Discussion

Previous studies have shown that FUS-mediated BBB opening affects cognitive functions; however, most of them were results for a short period of time, within 4 weeks after FUS treatment [6,30]. In addition, many studies have reported that FUS-mediated BBB opening in the hippocampus induces neurogenesis [6,8,22]. Adult hippocampal neurogenesis plays an important role in synaptic plasticity in the DG. As the DG is the core of afferent input to the hippocampus, synaptic plasticity and neurogenesis are closely related to hippocampal functions, such as memory and cognitive function [31,32]. We hypothesized that the cognitive improvement effect of FUS is due to LTP induced by changes in synaptic plasticity or neurogenesis. In this study, 5xFAD at 6–7 months of age were used, at which time neuronal loss occurred sufficiently and

A Training

B Sham · Sham + FUS · TG · TG + FUS

C Crossings

D Quadrant zone

E Platform zone

F Speed

G

H

I

(caption on next page)

Fig. 2. Restoration of memory impairment by FUS. FUS improves cognitive function and spatial memory after 6 weeks of treatment. **A,** earning curves of the five consecutive days. Latency to platform means the time required for mice to find the escape platform during training trials. Two-way ANOVA with Fisher's LSD multiple comparison test. Data are presented means ± standard error of the mean (SEM). *$p < 0.05$, **$p < 0.01$ TG compared to Sham, #$p < 0.05$, ##$p < 0.01$ TG compared to Sham + FUS, @$p < 0.05$ TG compared to TG + FUS. **B,** Trajectory maps of animals in the probe test. **C–F,** Results of the probe test one day after the end of the training for five days. One-way ANOVA with Tukey's multiple comparison test. Data are presented means ± SEM. *$p < 0.05$, **$p < 0.01$, ***$p < 0.001$, ****$p < 0.0001$. **G,** Y-maze spontaneous alternation test. **H,** The rate of alteration in the Y-maze was recorded. **I,** The total number of arm entries in the Y-maze was evaluated. One-way ANOVA with Tukey's multiple comparison test. Data are presented means ± SEM. *$p < 0.05$, **$p < 0.01$, ***$p < 0.001$, ****$p < 0.0001$.

cognitive function began to decline. In addition, massive Aβ accumulation, which is the biggest pathological feature of AD, is observed. We observed changes after 6 weeks of FUS sonication because it takes approximately 3–4 weeks for neural progenitor cells to become mature neurons by FUS treatment; therefore, the time when the neuronal function of these mature neurons becomes active was considered to be at least 6 weeks [33–35].

Here, we report that AD is associated with cognitive impairment due to hippocampal changes and that this impairment could be reversed by FUS. In addition, FUS restored LTP levels in 8-month-old mice compared to those observed in sham and naïve adult mice. This LTP-enhancing effect of FUS was observed in the reduction in SC-CA1 synapse LTP, which is associated with disease progression. Dementia reduces NMDAR-dependent LTP, and changes in LTP, together with an increased tendency for synaptic depression, contribute to impaired memory functions observed in physiological aging [36,37]. Therefore, it is important to explore ways to restore LTP levels to those observed in young and late-middle-aged mice. In our experiments, we demonstrated that FUS-induced increase in LTP increased SC-CA1 LTP to a magnitude similar to that in sham adult brain slices. These findings imply FUS-induced improvements in hippocampal LTP in patients with AD. Prior to hippocampal neurogenesis, the initial steps to restore hippocampal LTP are mediated by FUS.

In this study, it was confirmed that FUS-mediated BBB opening could restore cognitive function in 5xFAD mice. Interestingly, the Sham + FUS group spent significantly more time in the target quadrant zone of the probe test than the Sham group (Fig. 2D). Since it is known that FUS-mediated BBB opening induces adult hippocampal neurogenesis, we think that this effect can be sufficiently exhibited even under normal conditions [7,8]. Although the exact mechanism for this has not yet been elucidated, it is thought that it might be closely related to upregulation of brain-derived neurotrophic factor (BDNF) [38–40] or various environmental vascular changes [4,41], which might have affected cognitive improvement. Activation of certain signaling pathways, including the Wnt/β-catenin, PI3K/Akt, and BDNF/TrkB/CREB pathways, plays a crucial role in promoting adult hippocampal neurogenesis in AD [42, 43]. These pathways have promising potential as a novel therapeutic strategy for AD. Therefore, it will be more persuasive to consider the convergence of these signaling pathways and molecules when presenting the neurogenesis effect through FUS-mediated BBB opening in the future.

FUS-mediated BBBO reduces Aβ in AD mice model [10,11,44,45], and has been reported to last for approximately 2 weeks [9]. In this study, Aβ accumulation was quantified by sacrificing the mice after 7 weeks of FUS treatment. There was no significant difference in Aβ accumulation between the TG + FUS and TG groups. Although Aβ levels decreased after FUS treatment, it was thought to have increased over 7 weeks. Although Aβ was not reduced, the recovery of cognitive function and induction of LTP suggest that Aβ accumulation may not be directly related to cognitive function. The BBB opening might not eliminate Aβ plaques; however, it is very important to note that after FUS treatment, the long-lasting effect of memory restoration is maintained even after 6 weeks of treatment. This means that there may be other mechanisms to restore hippocampal LTP. The repair of impaired cognitive functions might not be a route of pathological mechanism, yet it is implicative that the different mechanisms are inter-related, yet the cascading effects of repair mechanisms play a role in restoring memory deficits. The permanent damage of the memory sections in the hippocampus may not be

changed, but the newly synthesized neurons and synapses can restore the original functions of the hippocampus.

In this study, we first reported that neurodegenerative diseases can be treated by modulating the brain anatomy using non-invasive methods such as FUS to mildly alter the structures of the closely organized tissue in order to find a way to restore deteriorated hippocampal memory functions. As mentioned earlier, the synaptic plasticity of the hippocampus can be easily molded; however, it is unclear how FUS mediates the increase in SC-CA1 LTP in AD. Our study clearly confirmed the mechanism of cognitive improvement through FUS by confirming LTP induction. We revealed changes in LTP by FUS-mediated BBBO for the first time in an AD model of neurodegenerative disease, which is considered very meaningful results in that it lasts more than 6 weeks after only one treatment.

This study has limitations in that we measured LTP following FUS only at 6-week but it needs to be further measured at different timepoints, 2-week or 4-week. To better understand the role of LTP or cognitive function by FUS, we further need to investigate changes in neurogenesis or dendritic spine.

In summary, the main factor for cognitive improvement by FUS is thought to be enhanced neural plasticity rather than the reduction of Aβ plaques. In addition, since we confirmed that the effect of neural plasticity lasted close to 2 months, our results are thought to be helpful in setting treatment intervals of FUS. Considering that the reduction effect of Aβ plaques did not appear after 7 weeks of FUS treatment suggests that it is important to set the target of FUS treatment on neural plasticity rather than Aβ clearance, and further studies are needed.

Although the Alzheimer's disease mouse model has low LTP induction, FUS-mediated BBB opening obviously induced LTP recovery, which is associated with learning and memory and may affect the recovery of impaired cognitive function. These results imply that FUS contributes to the recovery of BBB permeability deficits by restoring the decreased hippocampal activity in AD.

5. Conclusion

In conclusion, we demonstrated that FUS effectively improved the dysfunctions associated with AD through synaptic plasticity. Overall, our findings suggest that FUS might serve as a potential therapeutic agent to improve cognitive deficits induced by Alzheimer's diseases.

CRediT authorship contribution statement

Chanho Kong: carried out all experiments except for electrophysiology, Formal analysis, All electrophysiological experiments and analyzes were performed, Writing – original draft, wrote the manuscript, All authors read and approved the final manuscript. **Ji Woong Ahn:** carried out all experiments except for electrophysiology, Formal analysis, All electrophysiological experiments and analyzes were performed, All authors read and approved the final manuscript. **Sohyun Kim:** carried out
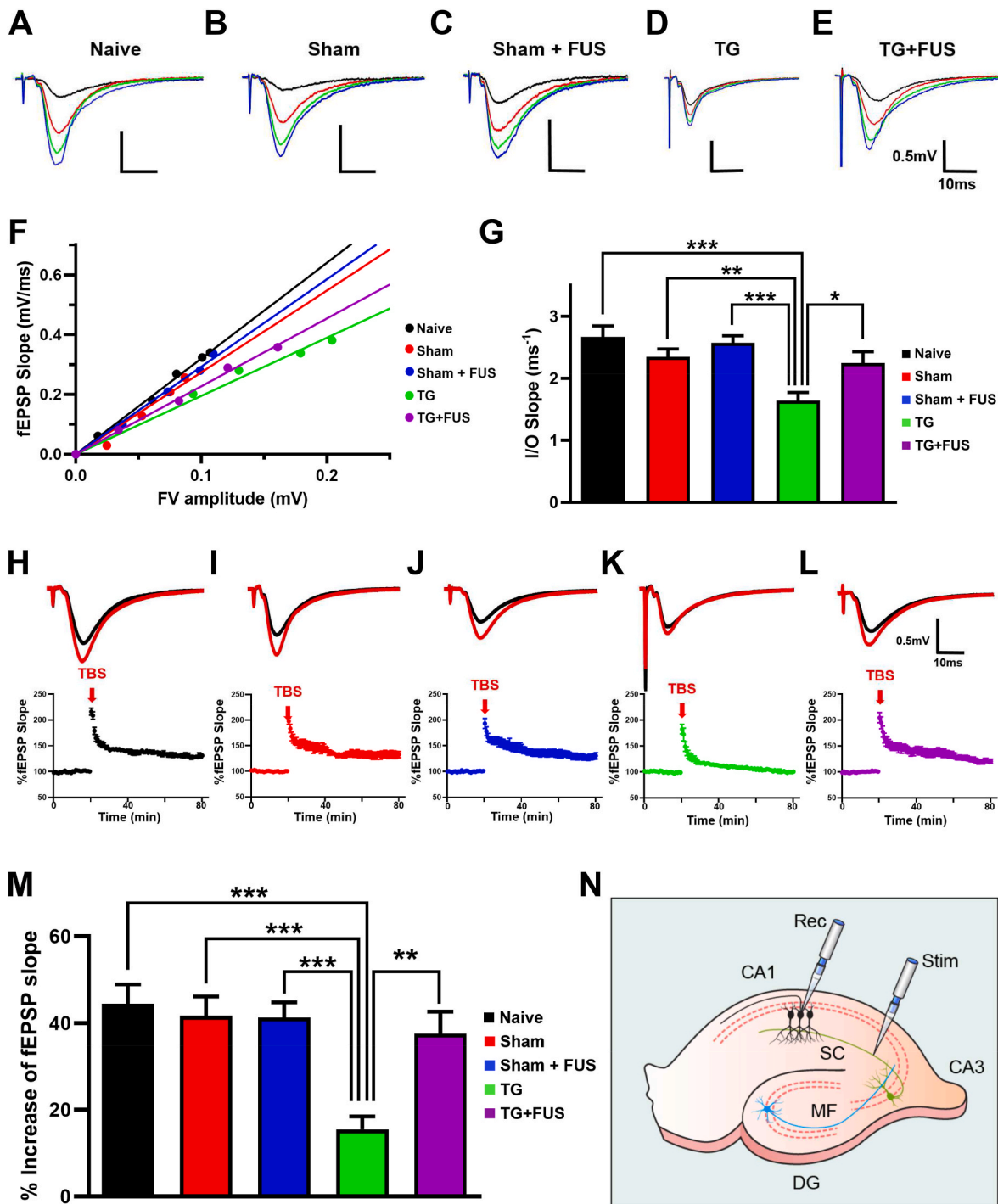
Fig. 3. Changes the synaptic strength and LTP. A-E, Representative traces of fEPSPs from hippocampal slices from representative experiments at four increasing stimulus intensities. **F,** The scatter plot of the Input and Output (I/O) relationship corresponding to the recorded fEPSPs in a-e. G, The average of slope I/O relationship for Naïve, LM, LM + FUS, TG, and TG + FUS (Naïve: 2.7 ± 0.2, n = 10 slices/5 mice; LM: 2.4 ± 0.10, n = 11 slices/5 mice; LM + FUS: 2.6 ± 0.1, n = 11 slices/5 mice; TG: 1.6 ± 0.1, n = 12 slices/5 mice; TG + FUS: 2.3 ± 0.2, n = 9 slices/4 mice). **G,** I/O slope and % increase of fEPSP slope in FUS FUS restored LTP at Schaffer collateral-CA1 synapses in Alzheimer's mice. **H-L,** Top: Representative traces showing field EPSPs before (average of 20 traces, black line) and after (average of 180 traces, red line) high-frequency stimulus. Bottom: Average time courses for field EPSP amplitude during LTP induction in all groups. Data are shown as mean ± SEM. **M,** Quantified graph was shown (Naïve: 44.5 ± 4.5 = 10 slices/5 mice; LM: 110.0 ± 1.7, n = 11 slices/5 mice; LM + FUS: 41.3 ± 3.5, n = 12 slices/5 mice; TG: 15.5 ± 3.0, n = 11 slices/5 mice; TG + FUS: 37.6 ± 5.1, n = 10 slices/5 mice). Data are represented as mean ± SEM (One-way ANOVA Tukey's post hoc test, ***p < 0.001). N, Schematic diagram of Shaffer's collateral circuit in the hippocampus to record LTP. (For interpretation of the references to colour in this figure legend, the reader is referred to the Web version of this article.)
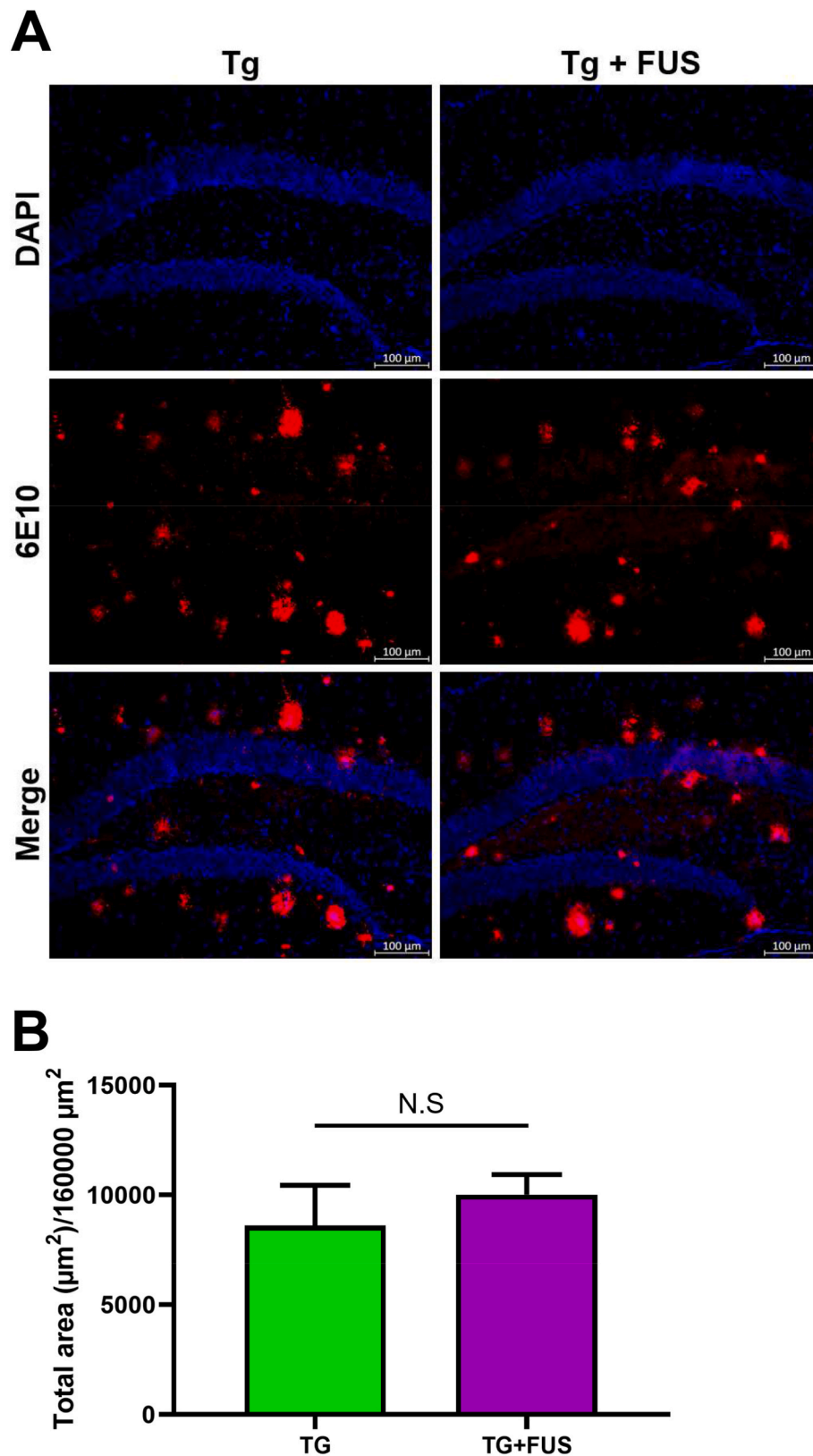
Fig. 4. Changes of the Aβ plaques. The effect of reducing Aβ plaques by FUS-mediated BBB opening does not last until 7 weeks. **A,** Representative images of the immunofluorescent staining in dentate gyrus of hippocampus for 6E10 antibody (Marker of Aβ plaque) and DAPI (Scale bar: 100 μm). **B,** Total area occupied by Aβ deposits in the dentate gyrus of hippocampus was measured for quantification (n = 4–5). Data was analyzed via unpaired t-test.

A

p-PKA (42 kDa)

t-PKA (42 kDa)

GAPDH (37 kDa)

B
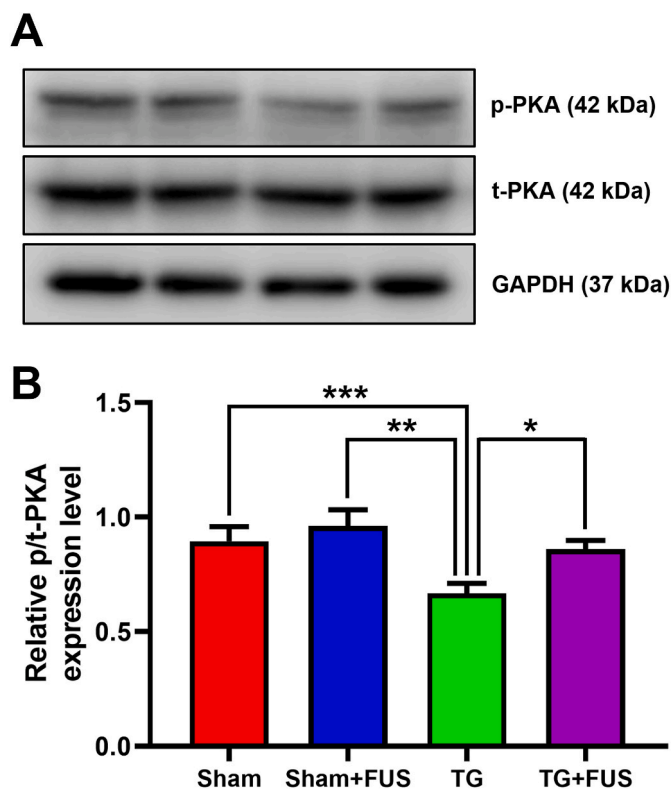
Fig. 5. Changes of the neural plasticity. A, Western blot analysis of phosphor PKA (p-PKA) and total PKA (t-PKA) levels in hippocampus. **B,** Bar graph showed marked increases in p-PKA/PKA levels in TG + FUS group relative to those in TG group was increased.

all experiments except for electrophysiology, Formal analysis, All electrophysiological experiments and analyzes were performed, Writing – original draft, wrote the manuscript, All authors read and approved the final manuscript. **Ji Young Park:** carried out all experiments except for electrophysiology, Formal analysis, All electrophysiological experiments and analyzes were performed, All authors read and approved the final manuscript. **Young Cheol Na:** critically revised the manuscript, All authors read and approved the manuscript. **Jin Woo Chang:** critically revised the manuscript, All authors read and approved the final manuscript. **Seungsoo Chung:** designed all experiments, All authors read and approved the final manuscript. **Won Seok Chang:** designed all experiments.

Declaration of competing interest

The authors declare that they have no known competing financial interests or personal relationships that could have appeared to influence the work reported in this paper.

Acknowledgements

Appendix A. Supplementary data

Supplementary data to this article can be found online at https://doi.org/10.1016/j.brs.2023.05.014.

References

[1] Hynynen K, McDannold N, Vykhodtseva N, Jolesz FA. Noninvasive MR imaging–guided focal opening of the blood-brain barrier in rabbits. Radiology 2001;220(3):640–6.

[2] McDannold N, Vykhodtseva N, Hynynen K. Targeted disruption of the blood–brain barrier with focused ultrasound: association with cavitation activity. Phys Med Biol 2006;51(4):793.

[3] Lee J, Chang WS, Shin J, Seo Y, Kong C, Song B-W, et al. Non-invasively enhanced intracranial transplantation of mesenchymal stem cells using focused ultrasound mediated by overexpression of cell-adhesion molecules. Stem Cell Res 2020;43:101726.

[4] McMahon D, Hynynen K. Acute inflammatory response following increased blood-brain barrier permeability induced by focused ultrasound is dependent on microbubble dose. Theranostics 2017;7(16):3989.

[5] Kovacs ZI, Kim S, Jikaria N, Qureshi F, Milo B, Lewis BK, et al. Disrupting the blood–brain barrier by focused ultrasound induces sterile inflammation. Proc Natl Acad Sci USA 2017;114(1):E75–84.

[6] Shin J, Kong C, Lee J, Choi BY, Sim J, Koh CS, et al. Focused ultrasound-induced blood-brain barrier opening improves adult hippocampal neurogenesis and cognitive function in a cholinergic degeneration dementia rat model. Alzheimer's Res Ther 2019;11(1):1–15.

[7] Scarcelli T, Jordão JF, O'reilly MA, Ellens N, Hynynen K, Aubert I. Stimulation of hippocampal neurogenesis by transcranial focused ultrasound and microbubbles in adult mice. Brain Stimul 2014;7(2):304–7.

[8] Mooney SJ, Shah K, Yeung S, Burgess A, Aubert I, Hynynen K. Focused ultrasound-induced neurogenesis requires an increase in blood-brain barrier permeability. PLoS One 2016;11(7):e0159892.

[9] Jordão JF, Thévenot E, Markham-Coultes K, Scarcelli T, Weng Y-Q, Xhima K, et al. Amyloid-β plaque reduction, endogenous antibody delivery and glial activation by brain-targeted, transcranial focused ultrasound. Exp Neurol 2013;248:16–29.

[10] Leinenga G, Götz J. Scanning ultrasound removes amyloid-β and restores memory in an Alzheimer's disease mouse model. Sci Transl Med 2015;7(278). 278ra33-ra33.

[11] Poon CT, Shah K, Lin C, Tse R, Kim KK, Mooney S, et al. Time course of focused ultrasound effects on β-amyloid plaque pathology in the TgCRND8 mouse model of Alzheimer's disease. Sci Rep 2018;8(1):1–11.

[12] Lipsman N, Meng Y, Bethune AJ, Huang Y, Lam B, Masellis M, et al. Blood–brain barrier opening in Alzheimer's disease using MR-guided focused ultrasound. Nat Commun 2018;9(1):1–8.

[13] Rezai AR, Ranjan M, D'Haese P-F, Haut MW, Carpenter J, Najib U, et al. Noninvasive hippocampal blood– brain barrier opening in Alzheimer's disease with focused ultrasound. Proc Natl Acad Sci USA 2020;117(17):9180–2.

[14] Park SH, Baik K, Jeon S, Chang WS, Ye BS, Chang JW. Extensive frontal focused ultrasound mediated blood–brain barrier opening for the treatment of Alzheimer's disease: a proof-of-concept study. Transl Neurodegener 2021;10(1):1–11.

[15] Gotz J, Chen Fv, Van Dorpe J, Nitsch R. Formation of neurofibrillary tangles in P301L tau transgenic mice induced by Aβ42 fibrils. Science 2001;293(5534):1491–5.

[16] Lewis J, Dickson DW, Lin W-L, Chisholm L, Corral A, Jones G, et al. Enhanced neurofibrillary degeneration in transgenic mice expressing mutant tau and APP. Science 2001;293(5534):1487–91.

[17] Walsh DM, Klyubin I, Fadeeva JV, Cullen WK, Anwyl R, Wolfe MS, et al. Naturally secreted oligomers of amyloid β protein potently inhibit hippocampal long-term potentiation in vivo. Nature 2002;416(6880):535–9.

[18] Jordao JF, Ayala-Grosso CA, Markham K, Huang Y, Chopra R, McLaurin J, et al. Antibodies targeted to the brain with image-guided focused ultrasound reduces amyloid-β plaque load in the TgCRND8 mouse model of Alzheimer's disease. PLoS One 2010;5(5):e10549.

[19] Alecou T, Giannakou M, Damianou C. Amyloid β plaque reduction with antibodies crossing the blood-brain barrier, which was opened in 3 sessions of focused ultrasound in a rabbit model. J Ultrasound Med 2017;36(11):2257–70.

[20] Xhima K, Markham-Coultes K, Nedev H, Heinen S, Saragovi H, Hynynen K, et al. Focused ultrasound delivery of a selective TrkA agonist rescues cholinergic function in a mouse model of Alzheimer's disease. Sci Adv 2020;6(4):eaax6646.

[21] Xhima K, Markham-Coultes K, Hahn Kofoed R, Saragovi HU, Hynynen K, Aubert I. Ultrasound delivery of a TrkA agonist confers neuroprotection to Alzheimer-associated pathologies. Brain 2022;145(8):2806–22.

[22] Dubey S, Heinen S, Krantic S, McLaurin J, Branch DR, Hynynen K, et al. Clinically approved IVIg delivered to the hippocampus with focused ultrasound promotes neurogenesis in a model of Alzheimer's disease. Proc Natl Acad Sci USA 2020;117(51):32691–700.

[23] Karakatsani ME, Kugelman T, Ji R, Murillo M, Wang S, Niimi Y, et al. Unilateral focused ultrasound-induced blood-brain barrier opening reduces phosphorylated tau from the rTg4510 mouse model. Theranostics 2019;9(18):5396.

[24] Pandit R, Leinenga G, Götz J. Repeated ultrasound treatment of tau transgenic mice clears neuronal tau by autophagy and improves behavioral functions. Theranostics 2019;9(13):3754.

[25] Shin J, Kong C, Cho JS, Lee J, Koh CS, Yoon M-S, et al. Focused ultrasound–mediated noninvasive blood-brain barrier modulation: preclinical examination of efficacy and safety in various sonication parameters. Neurosurg Focus 2018;44(2):E15.

[26] Burgess A, Dubey S, Yeung S, Hough O, Eterman N, Aubert I, et al. Alzheimer disease in a mouse model: MR imaging–guided focused ultrasound targeted to the hippocampus opens the blood-brain barrier and improves pathologic abnormalities and behavior. Radiology 2014;273(3):736–45.

[27] Kong C, Yang E-J, Shin J, Park J, Kim S-H, Park S-W, et al. Enhanced delivery of a low dose of aducanumab via FUS in 5× FAD mice, an AD model. Transl Neurodegener 2022;11(1):57.

[28] Whitlock JR, Heynen AJ, Shuler MG, Bear MF. Learning induces long-term potentiation in the hippocampus. science 2006;313(5790):1093–7.

[29] Lynch MA. Long-term potentiation and memory. Physiol Rev 2004;84(1):87–136.

[30] Burgess A, Dubey S, Yeung S, Hough O, Eterman N, Aubert I, et al. Alzheimer disease in a mouse model: MR imaging–guided focused ultrasound targeted to the hippocampus opens the blood-brain barrier and improves pathologic abnormalities and behavior. Radiology 2014;273(3):736.

[31] Snyder J, Kee N, Wojtowicz J. Effects of adult neurogenesis on synaptic plasticity in the rat dentate gyrus. J Neurophysiol 2001;85(6):2423–31.

[32] Bruel-Jungerman E, Rampon C, Laroche S. Adult hippocampal neurogenesis, synaptic plasticity and memory: facts and hypotheses. Rev Neurosci 2007;18(2):93–114.

[33] Kristiansen M, Ham J. Programmed cell death during neuronal development: the sympathetic neuron model. Cell Death Differ 2014;21(7):1025–35.

[34] Gonçalves JT, Schafer ST, Gage FH. Adult neurogenesis in the hippocampus: from stem cells to behavior. Cell 2016;167(4):897–914.

[35] Niklison-Chirou MV, Agostini M, Amelio I, Melino G. Regulation of adult neurogenesis in mammalian brain. Int J Mol Sci 2020;21(14):4869.

[36] Min SS, Quan HY, Ma J, Han J-S, Jeon BH, Seol GH. Chronic brain inflammation impairs two forms of long-term potentiation in the rat hippocampal CA1 area. Neurosci Lett 2009;456(1):20–4.

[37] Forner S, Baglietto-Vargas D, Martini AC, Trujillo-Estrada L, LaFerla FM. Synaptic impairment in Alzheimer's disease: a dysregulated symphony. Trends Neurosci 2017;40(6):347–57.

[38] Patterson SL, Abel T, Deuel TA, Martin KC, Rose JC, Kandel ER. Recombinant BDNF rescues deficits in basal synaptic transmission and hippocampal LTP in BDNF knockout mice. Neuron 1996;16(6):1137–45.

[39] Tufail Y, Matyushov A, Baldwin N, Tauchmann ML, Georges J, Yoshihiro A, et al. Transcranial pulsed ultrasound stimulates intact brain circuits. Neuron 2010;66(5):681–94.

[40] Henry RA, Hughes SM, Connor B. AAV-mediated delivery of BDNF augments neurogenesis in the normal and quinolinic acid-lesioned adult rat brain. Eur J Neurosci 2007;25(12):3513–25.

[41] McMahon D, Bendayan R, Hynynen K. Acute effects of focused ultrasound-induced increases in blood-brain barrier permeability on rat microvascular transcriptome. Sci Rep 2017;7(1):1–15.

[42] Liu H, Zhang H, Ma Y. Molecular mechanisms of altered adult hippocampal neurogenesis in Alzheimer's disease. Mechanisms of ageing and development 2021;195:111452.

[43] Jia L, Piña-Crespo J, Li Y. Restoring Wnt/β-catenin signaling is a promising therapeutic strategy for Alzheimer's disease. Mol Brain 2019;12:1–11.

[44] Leinenga G, Götz J. Safety and efficacy of scanning ultrasound treatment of aged APP23 mice. Front Neurosci 2018;12:55.

[45] Leinenga G, Koh WK, Götz J. Scanning ultrasound in the absence of blood-brain barrier opening is not sufficient to clear β-amyloid plaques in the APP23 mouse model of Alzheimer's disease. Brain Res Bull 2019;153:8–14. https://doi.org/10.1016/j.brainresbull.2019.08.002.